https://dx.doi.org/10.1016/j.engstruct.2019.110051

Experimental Evidence on Structural Adequacy of High Strength S690 Steel Welded Joints with Different Heat Input Energy

Kwok-Fai Chung[1,2*], Ho-Cheung Ho[1,2] , Yi-fei Hu[1,2], Kai Wang[1,2], Xiao Lui[1,2], Meng Xiao[1,2] and David A. Nethercot [1,3]

[1]*Department of Civil and Environmental Engineering, The Hong Kong Polytechnic University, Hong Kong SAR, China.*

[2] *Chinese National Engineering Research Centre for Steel Construction (Hong Kong Branch) The Hong Kong Polytechnic University, Hong Kong SAR, China.*

[3] *Department of Civil and Environmental Engineering, Imperial College London, U.K.*

** Corresponding author: kwok-fai.chung@polyu.edu.hk*

ABSTRACT

Quenching and tempering is a highly developed heat treatment method to produce high strength steels with certain quantities of expensive alloy elements. This process has been highly industrialized and widely adopted in modern steel mills to produce high strength S690 steels. However, a heating / cooling cycle induced during welding may initiate phase transformation, re-crystallization and grain growth in microstructures of these steels. This will cause significant reduction in their mechanical properties if both the maximum temperatures during welding and the cooling rates after welding are not properly controlled. Over the past twenty years, conflicting research findings have been reported on mechanical properties of these S690 welded sections due to different welding procedures and parameters adopted during welding.

In order to quantify adverse effects on mechanical properties of the S690 steel welded joints, a series of pilot tests on a total of 18 coupons of S690 steel plates, welded joints and weld metals with different heat input energy during welding have been conducted to examine their deformation characteristics under tension. Moreover, 12 reference and 12 spliced S690 welded H-sections with different heat input energy adopted in the welding processes have been conducted to examine their deformation characteristics under compression, in particular, their section resistances under compression. It is demonstrated that by a proper control on the heat input energy during welding, it is possible to control or even eliminate any reduction in the mechanical properties of these S690 welded joints under either tension or compression. Consequently, experimental evidence on structural adequacy of these high strength S690 steel welded joints with different heat input energy adopted in the welding processes is provided scientifically to confirm applications of these high strength S690 steel in construction.

Keywords: High strength steels; welding; microstructure change; reduction in mechanical properties; heat input energy.

1. Introduction

High strength S690 steels are efficient steel products which possess mechanical strengths two to three times to those of normal strength steels, such as S235 and S355 steels. Owing to their excellent strength-to-self weight ratios, they are highly desirable to be used in heavily loaded structures, leading to a potential saving in both materials and costs in the order of 30 to 50 %. Since 2000, high strength steels have been successfully used in large lifting equipment, machinery and offshore structures. However, they have not been widely adopted in construction owing to potential adverse effects of welding on their microstructures which lead to significant reductions in their mechanical properties [1]. Hence, it is necessary to examine structural adequacy of these S690 welded joints with different heat input enegry in order to ensure satisfcatory structural performance of S690 welded members in construction.

1.1 Adverse effects of welding onto high strength steels

In general, welding in normal strength S355 steels does not cause any significant strength reduction as they are primarily ferritic or ferritic-pearlitic steels which microstructures do not undergo phase transformation during welding. However, high strength steels are primarily manufactured with heat treatments during steel-making [5], such as Quenching and Tempering for QT steels, so that they can attain specific martensitic-ferritic microstructures. These high strength steels possess highly favourable properties of strength, ductility and toughness. However, large heating/cooling cycles induced during a practical welding process will trigger phase transformation, recrystallization and grain growth in heat-affected-zones (HAZ) of their welded joints as shown in Figure 1. Depending on chemical compositions of the steels, the maximum temperatures reached during welding, T_{max} , and the time for cooling after welding from 800 to 500 $^{\circ}$C, $t_{8/5}$, as shown in Figure 2, various phases of the QT steels will be formed. Hence, significant adverse effects on mechanical properties of these welded joints at locations within the HAZ, in particular, hardness (i.e. softening), will be resulted, if the heat input energy, q (kJ/mm), adopted during welding is not properly controlled [6].

1.2 Materials research into high strength steels

Over the past three decades, materials scientists and researchers on metallurgy developed various methods to conduct microstructure characterization in different types of steels, or more precisely, different phases of steels with different volumetric fractions based on different combinations of chemicals and heat treatments. These methods include dilatometry tests, Vickers hardness measurements, and three dimensional micro-polycrystal structural analyses using scan electronic microscopes (SEM) and electron backscattering diffraction color coding (EBSD) to estimate volume fractions of various phases of recrystallized steels [7, 8]. It should be noted that both the composition and the variety of different phases of the recrystallized steels within the HAZ of a S690 welded joint depend heavily on evolution of microstructures of the steel plates during the heating / cooling process of welding. Through both SEM and EBSD analyses, the grain sizes and the orientations of various phases of the recrystallized steels can

be readily identified respectively. According to the curves obtained by dilatometry tests, which are widely employed to measure critical transformation temperatures, different phases of the recrystallized steels are classified using a lever rule [9,10].

In order to determine mechanical properties of the HAZ in the S690 welded joints, it is important to understand the phase transformation mechanism of these steels due to typical heating / cooling process under practical welding. Reduction in mechanical properties of S690 welded joints due to changes in microstructures [11] have also been examined and reported extensively. Moreover, such changes in microstructures in these welded joints had been investigated systematically by Mayr, Ding et al., and Azhari et al. [12~14]. These materials researchers had carried out systematic experimental and numerical investigations to correlate mechanical properties of these HAZ using high-fidelity micro-mechanical models and meso-scale mechanical analyses [15, 16]. It should be noted that the primary interests of these material researchers are to understand, and then, to characterize microstructures and their re-crystallization conditions so that they are able to develop a variety of high performance steels with different and probable less expensive chemicals. Hence, their interests are different from those of the international communities of structural engineering and steel construction, i.e. how to apply these high strength steels efficiently and reliably in construction.

1.3 Related investigations on high strength S690 steel plates and their welded sections

In order to promote effective use of the high strength S690 steels in construction, it is essential to examine mechanical properties and structural behaviour of the S690 steel members and their joints. A comprehensive research programme on experimental and numerical investigations was conducted by the authors on i) mechanical properties of the S90 steels and their welded sections under monotonic and cyclic actions [17~19], ii) cross-sectional resistances of welded S690 H-sections as stocky columns [20], iii) member resistances of welded S690 H-sections as slender columns [21~23], and iv) cross-sectional and member resistances of welded S690 I-sections as restrained and unrestrained beams respectively [24].

However, it becomes obvious in many cases that reductions in various mechanical properties of these high strength S690 steel welded joints are found to be significantly less severe than anticipated [14~16]. In general, there is a lack of systematic experimental evidence on such reduction on the mechanical properties of these S690 steel welded joints as well as on the structural behaviour of these S690 steel members.

1.4 Objectives and scope of work

In order to promote effective use of high strength S690 steel members in construction, a comprehensive experimental investigation is undertaken to examine mechanical properties of welded joints and structural behaviour of high strength S690 steel welded H-sections. It aims to quantify mechanical properties of both steel plates and their welded joints manufactured with different heat

input energy during welding (but with no control during cooling), and hence, to establish whether there are significant reductions in the mechanical properties of the S690 welded joints and sections. More importantly, it is necessary to demonstrate that these high strength S690 steels can be used efficiently and reliably in construction with properly controlled welding.

The project takes the following forms of experimental investigation:

- Pilot tests: Tensile tests on coupons of S690 steel welded joints
  A total of 18 standard tensile tests are carried out on coupons of S690 steel plates and their welded joints as well as weld metals with various heat input energy, q. After data analyses, deformation characteristics of these coupons under tension are obtained.

- Compression tests on stocky columns of S690 reference welded H-sections
  A total of 12 compression tests are carried out on stocky columns of S690 steel welded H-sections, i.e. a total of four section sizes, namely, Sections C1, C2, C3 and C4 with a practical range of plate thicknesses and section sizes. Deformation characteristics of these S690 steel welded H-sections under compression are obtained as reference data for subsequent comparisons.

- Compression tests on stocky columns of S690 spliced welded H-sections
  A total of 12 compression tests are also carried out on stocky columns of S690 steel welded H-sections, also of four different section sizes, with butt welded joints, i.e. column splices, at mid-height with various heat input energy, q. Deformation characteristics of these S690 spliced welded H-sections under compression are obtained for direct comparison with those reference data obtained above.

Key areas of interest of the investigation are:

a) deformation characteristics of S690 steel welded joints with different heat input energy q during welding under i) tension, and ii) compression; and
b) any reduction on the mechanical properties of S690 steel welded joints due to welding.

It should be noted that these experimental investigations have been conducted over a period of 3 years, and mechanical properties of different batches of 6, 10 and 16 mm thick S690 steel plates are provided. In order to ensure high as well as consistent welding quality, both a robotic welding system (for GMAW) and an automated welding machine (for SAW) are employed during manufacturing of test specimens of the pilot tests. Based on established welding procedures and parameters developed in the pilot tests, all the reference and the spliced welded H-sections are fabricated by highly skilled welders. In general, even- or over-match welding is adopted during welding of all these sections in order to avoid unexpected failure, and Table 1 summarizes material specifications of both the S690 steel plates and the welding materials adopted in the investigation.

Table 2 provides details of the welding procedures and parameters for both fillet and butt welds adopted in these test specimens.

2 Pilot Tests

In order to investigate and quantify effects of various heat input energy onto the mechanical properties of the S690-QT steel welded joints under tension, a series of carefully planned and executed standard tensile tests on cylindrical coupons of the welded joints were conducted [15,16]. Table 3 summarizes the test programme in which a total of 18 standard cylindrical coupons, i.e. 3 coupons of the steel plates, 12 coupons of the welded joints, and 3 coupons of weld metal, were tested. It should be noted that four different heat input energy, q, are specified, namely, q = 1.0, 1.5, 2.0 and 5.0 kJ/mm, during welding. Figure 3 illustrates the process of robotic welding for preparation of butt welded joints between the S690 steel plates, the arrangements of various coupon types in the welded steel plates, and detailed dimensions of the coupons. Both the welding procedures and parameters are shown in Table 4. It should be noted that the heat input energy for GMAW at 2.0 kJ/mm is commonly considered to be a practical maximum, and hence, the heat input energy at 5.0 kJ/mm is achieved through the use of SAW.

It should be noted that all the coupons were machined and tested under monotonic tension forces according to BS EN ISO 6892-1 [26]. Strain gauges were attached to these coupons to measure strains accurately at small deformations while a digital photo imaging method was employed to determine strains at large deformations accurately through pixel measurement.

2.1 Test results

All the tests have been conducted successfully. It was shown that in almost all coupons of the welded joints tested, fracture occurred within the heat affected zones of the welded joints without any failure in neither the weld metal nor the base plates, as shown in Figure 4. Table 5a) summarizes various mechanical properties of these cylindrical coupons of the S690 steel plates and welded joints, and it is shown that the mechanical properties of these welded joints vary significantly according to the heat input energy q during welding. The engineering stress-strain curves of these welded joints are plotted onto the same graph in Figure 5 for direct comparison while reduction factors for various mechanical properties of these S690 welded joints are presented in Table 5b). It should be noted that

- the reduced yield strengths at 0.2 % proof strains of the welded coupons with q = 1.0, 1.5, 2.0 and 5.0 kJ/mm are found to be 0.98, 0.90, 0.86 and 0.70 of those of the steel plates respectively;
- similarly, the reduced tensile strengths of the welded coupons with q = 1.0, 1.5, 2.0 and 5.0 kJ/mm are found to be 1.00, 0.97, 0.92 and 0.83 of those of the steel plates respectively; and
- it is evident that reductions to various mechanical properties of the base plates due to the effect of welding are significant when q = 5.0 kJ/mm. However, when the values of q are small, there are relatively small reductions to the mechanical properties of the steel plates,

in particular, when q = 1.0 kJ/mm.

Consequently, it is successfully demonstrated that S690 steels are sensitive to the heating / cooling cycles during welding, and the heat input energy should be controlled carefully in order to produce welded joints with no or small reduction to their mechanical properties under tension when compared with those of the steel plates. Moreover, reduction factors to both the yield and the tensile strengths of these welded joints with different heat input energy under tension have been successfully quantified. Refer to Liu et al. [27] for further details.

3 Compression Tests on Stocky Columns of S690 Reference Welded H-sections

In order to obtain basic deformation characteristics of the S690 welded H-sections as reference, a total of 12 compression tests were carried out, and Table 6 summarizes the test programme. Figure 6 illustrates four welded H-sections with different cross-sectional dimensions, namely Sections C1 to C4, and steel plates with three different thicknesses, i.e. 6, 10 and 16 mm, are used in these sections. Table 1b) presents their mechanical properties obtained in standard coupon tests. It should be noted that three nominal identical welded H-sections were tested for each section size. The nominal heights of these stocky columns are assigned to be 3 times of their section depths so that i) local buckling is readily developed in both the flange and the web plates without significant end restraints, and ii) overall buckling does not take place because of their small overall slenderness.

Table 2a) presents various welding procedures and parameters adopted during fabrication of these Sections, and the heat input energy for single-pass fillet welding in the flange/web junctions is kept to be about 1.8 kJ/mm for Sections C1 and C2, and about 2.7 kJ/mm for Sections C3 and C4. It should be noted that a pre-heat temperature at 100 to 120 ºC is adopted before welding while the inter-pass temperatures are rigorously controlled not to exceed 200 ºC according to temperature measurements of an infrared camera.

According to the existing section classification rules given in EN 1993-1-1 [3], Sections C1 and C3 are classified as Class 1 and 2 sections respectively while both Sections C2 and C4 are classified as Class 3 sections. Hence, full cross-section resistances of these four Sections are expected to be readily mobilized though local plate buckling in their flange and web plates may take place after yielding within the sections. In general, these high strength S690 welded H-sections are expected to behave in many ways similar to those of S355 welded H-sections.

3.1 Test set-up, instrumentation and procedures

Two different testing systems are employed to conduct compression tests on various sections according to expected failure loads of these stocky columns. The testing systems are shown in Figure 7, i.e. Sections C1 and C2 are tested with a MTS Testing System with a loading capacity of 4,000 kN while Sections C3 and C4 are tested with a Hydraulic Servo Control Testing System with a loading

capacity of 10,000 kN. Both ends of the H-sections are properly welded onto thick end plates to ensure consistent deformations of the sections under compression.

Instrumentation of the compression tests is illustrated in Figure 8. Four strain gauges are attached to the flange tips of each test specimen at its mid-height to measure their axial strains. Four LVDTs are also installed to record relative shortenings between the two end plates. Moreover, the rate of force or displacement application in the tests are controlled to be very small in order to prevent any dynamic effect as follows:

- to increase an applied force equal to 30% of the predicted section resistance, $N_{c,Rd}$, and then, reduce the applied force back to zero at a rate of 300 kN/min;
- to increase the applied force up to 80% of $N_{c,Rd}$ at a rate of 200 kN/min;
- to continue the test through a displacement control at a rate of 0.5 mm/min; and
- to terminate the test when the applied force is reduced more than 20% of its maximum value after failure of the specimen.

3.2 Test results

All the tests have been conducted successfully. Typical deformed shapes of these reference welded H-sections after tests are shown in Figure 9. It should be noted that, in all cases, symmetrical local buckling appears in both flanges of these welded H-sections while complementary local buckling is also found in their web plates. Hence, the failure mode of these stocky columns is shown to be plastic local buckling in both the flange and the web plates of these H-sections. Figure 10 plots the measured applied load vs axial shortening curves of all these reference sections onto the same graph for easy comparison. It is evident that all these curves extend above the respective design section resistances $N_{c,Rd}$ of these Sections. All Sections C1S and C3S exhibit significant deformation ductility under compression, but there is little ductility in all Sections C2S and C4S. This agrees with the section classification obtained in accordance with the current classification rules for welded cross-sections given in EN 1993-1-1.

Table 7 presents the measured section resistances of all these S690 reference welded H-sections, $N_{c,Rt}$, together with their design resistances, $N_{c,Rd}$. The design resistances of the welded H-sections are given by:

$$N_{c,Rd} = 2 f_{y,f} \times b \times t_f + f_{y,w} \times (h - 2 \times t_f) \times t_w \qquad \text{(Eq. 1)}$$

where

$f_{y,f}$ and $f_{y,w}$ are the measured yield strengths of the flange and the web plates of the welded H-section respectively;

b and t_f are the measured width and the measured thickness of the flange plate of the welded H-section respectively; and

h and t_w are the measured overall depth and the measured thickness of the web plate of the welded H-section respectively.

It is shown that all the measured section resistances, $N_{c,Rt}$, are larger than the design section resistances, $N_{c,Rd}$, and the ratios of $N_{c,Rt}$ to $N_{c,Rd}$ range from 1.01 to 1.08 with an average value of 1.05. Hence, the current design rules given in EN 1993-1-1 [3] are able to predict the section resistances of these stocky columns of S690 welded H-sections under compression.

4 Compression tests on stocky columns of S690 spliced welded H-sections

In order to assess any adverse effect of welding onto structural behavior of the S690 welded H-sections, a total of 12 compression tests on Sections C1 to C4 with butt welded joints at mid-height, i.e. S690 spliced welded H-sections, were carried out. Table 8 summarizes the test programme. Figure 6 illustrates these four welded H-sections with different cross-sectional dimensions, and steel plates with three different thicknesses, i.e. 6, 10 and 16 mm, are used in these sections. Table 1b) presents their mechanical properties obtained in standard coupon tests. It should be noted that in this test series, only three different values of the heat input energy q are adopted during welding of the butt welded joints, i.e. q = 1.0, 1.5 and 2.0 kJ/mm, and the value of 5.0 kJ/mm is not adopted due to practical consideration. Refer to Table 2 for various welding procedures and parameters adopted during both fillet and butt welding of these sections.

It should be noted that all the test set-up, instrumentation and procedures are similar to those adopted in the compression tests on the reference welded H–sections described in Sections 3.1.

4.1 Test results

All the tests have been conducted successfully. Typical deformed shapes of these spliced welded H-sections after tests are shown in Figure 11. It should be noted that, in all cases, symmetrical local buckling appears in both flanges of these spliced welded H-sections while complementary local buckling is also found in their web plates. Hence, the failure mode of these stocky columns is shown to be plastic local buckling in both the flange and the web plates of these H-sections, i.e. similar to those of the reference welded H-sections.

The measured applied load vs axial shortening curves of all these spliced sections are plotted onto the same graph in Figure 12 for easy comparison. It is evident that all these curves extend above the respective design section resistances $N_{c,Rd}$ of these Sections. All Sections C1S and C3S exhibit significant deformation ductility under compression, but there is little ductility in all Sections C2S and C4S. This agrees with the section classification obtained in accordance with the current classification rules for welded cross-sections given in EN 1993-1-1.

Table 9 presents the measured section resistances of all these S690 spliced welded H-sections, $N_{c,Rt}$, together with their design section resistances, $N_{c,Rd}$ determined with Eq.(1) shown above. It is shown that all the measured section resistances, $N_{c,Rt}$, are larger than the design section resistances, $N_{c,Rd}$, and the ratios of $N_{c,Rt}$ to $N_{c,Rd}$ range from 1.02 to 1.11 with an average value of 1.06. Hence, there

is no reduction in the section resistances of these spliced welded H-sections when the heat input energy q adopted during welding ranges from 1.0 to 2.0 kJ/mm. Consequently, Eq.(1) is shown to be equally applicable to predict the section resistances of these stocky columns of S690 spliced welded H-sections under compression as no reduction to their section resistances is needed.

5 Comparison on deformation characteristics of S690 steels after welding

An overall comparison on the deformation characteristics of these S690 welded joints with different heat input energy under i) tension, and ii) compression is presented in the following sections.

5.1 S690 welded joints under tension

The test results of the welded coupons under tension obtained from the pilot tests described in Section 3 is considered as the deformation characteristics of these S690 welded joints with different heat input energy under tension. It should be noted that:

- As shown in the engineering stress-strain curves of these tensile tests with different levels of non-linearity, the reduction factors to the yield strengths of these welded joints under tension are shown to be 0.98, 0.90, 0.86 and 0.70 for q = 1.0, 1.5, 2.0 and 5.0 kJ/mm respectively. The corresponding reduction factors to the tensile strengths, and hence, the section resistances of these welded joints are shown to be 1.00, 0.97, 0.92 and 0.83 for q = 1.0, 1.5, 2.0 and 5.0 kJ/mm respectively.
- Such reductions may be explained with a significant change in microstructure within the heat affected zones (HAZ) of the welded joints with different heat input energy, and hence, the deformation characteristics of these coupons of welded joints under tension are very different among themselves.

5.2 S690 welded joints under compression

The test results of both the S690 reference and the S690 spliced welded H-sections under compression described in Sections 3 and 4 are considered together. It should be noted that:

- In order to allow for effective comparison, all the measured deformation characteristics curves of both the reference and the spliced welded H-sections are normalized with respective to their section resistances, $N_{c,Rd}$, and their corresponding axial shortenings Δ_o , and both the normalized resistance parameter, n and the normalized deformation parameter, η , are defined as shown in Figure 13. The normalized deformation characteristics (or the n-η curves) of each set of Sections C1 to C4 with as well as without butt welds at mid-heights are plotted onto various graphs in Figure 14 for easy comparison.
- It is evident from the n-η curves of the reference welded H-sections (without butt welds) that full section resistances are readily mobilized in all these 12 reference sections.
- According to the n-η curves of the spliced welded H-sections (with butt welds), full section resistances are also readily mobilized in all these 12 spliced sections despite the presence of butt welded joints at mid-height of the sections.

- Although these butt welded joints are made with different heat input energy, and hence, they have different combinations of microstructures in the vicinity of the heat-affected zones, there is no significant difference among the normalized deformation characteristics of these spliced sections under compression.

  This may be explained by the fact that the section resistances of these welded H-sections correspond to excessive plastic deformations, rather than elastic deformations, and hence, full section resistances are readily mobilized in these welded joints under compression, despite the presence of different microstructures in the HAZ of the welded joints.

As shown in Figure 13, Δ_f denotes the measured axial shortening of the stocky column at which its resistance under compression, after certain deformation, is equal to $N_{c,Rd}$. Hence, this parameter may be readily considered as an indication to ductility of the section under compression. The averaged values of Δ_f / Δ_o or η_f of all the sections are summarized in Table 10, and it is shown that

- those S690 welded H-sections with large η_f , i.e. from 4.4 to 5.2, exhibit large ductility, and they are considered as Class 1 or 2 sections according to the current section classification rules of EN 1993-1-1; and
- those S690 welded H-sections with small η_f , i.e. from 1.9 to 2.4, exhibit limited ductility, and they are considered as Class 3 sections according to the current section classification rules.

In both cases, the presence of butt welds at mid-height of the sections is shown to have negligible effects on the ductility of these S690 welded H-sections.

6 Conclusions

In order to quantify adverse effects on mechanical properties of the S690 steel welded joints, a series of pilot tests on a total of 18 coupons of S690 steel plates, welded joints and weld metals with different heat input energy during welding have been conducted to examine their deformation characteristics under tension. Moreover, 12 reference and 12 spliced S690 welded H-sections with different heat input energy adopted in the welding processes have been conducted to examine their deformation characteristics, in particular, their section resistances, under compression. Details of all the test programmes, and the corresponding test set-up, instrumentation and procedures are fully described.

It should be noted that all the test results, including the failure modes, the measured deformation characteristics, and the measured section resistances of the test specimens are presented in this paper. Moreover, these results are compared systematically to quantify any significant reduction in the mechanical properties of these S690 welded joints due to the effects of welding. It is demonstrated that by a proper control on the heat input energy during welding, it is possible to control or even eliminate any reduction in the mechanical properties of these S690 welded joints under either tension or compression. Consequently, experimental evidence on structural adequacy of these high strength

S690 steel welded joints with different heat input energy adopted in the welding processes is provided scientifically to confirm applications of these high strength S690 steel in construction.

ACKNOWLEDGEMENTS

The authors are grateful for the financial support provided by the Research Grants Council of the University Grants Committee of the Government of Hong Kong SAR (Project Nos. 152194/15E, 152687/16E, and 152231/17E). The projects leading to publication of this paper were also partially funded by the Chinese National Engineering Research Centre for Steel Construction (Hong Kong Branch) which is funded by the Innovation and Technology Commission of the Government of Hong Kong (Project No. BBY3), and the Research Committee of the Hong Kong Polytechnic University (Project Nos. BBY4 and BBY6). Moreover, the research studentships provided by the Research Committee of the Hong Kong Polytechnic University is acknowledged (Project Nos. RTK3, XXXX, XXXX).

All structural tests on high strength S690 steels were conducted at the Structural Engineering Research Laboratory of the Department of Civil and Environmental Engineering at the Hong Kong Polytechnic University, and supports from the technicians are gratefully acknowledged.

REFERENCES

[1] Willms R. (2009). High strength steel for steel construction. Proceedings of Nordic Steel Construction Conference, pp597-604.

[2] BS EN 10025-6. (2004). Hot Rolled Products of Structural Steels – Part 6: Technical delivery conditions for flat products of high yield strength structural steels in the quenched and tempered condition. British Standards Institution.

[3] CEN (2005). EN-1993-1-1:2005, Eurocode 3: Design of steel structures – Part 1–1: General rules and rules for buildings. European Committee for Standardization, Brussels, Belgium.

[4] CEN (2005). EN-1993-1-8:2005, Eurocode 3: Design of steel structures – Part 1–8: Design of joints. European Committee for Standardization, Brussels, Belgium.

[5] Krauss, G. (1980). Principles of heat treatment of steel. American Society for Metals.

[6] Easterling, KE. (1992). Introduction to the Physical Metallurgy of Welding 1992, Butterworth-Heinemann.

[7] Su B., Lin HP., Kuo JC., and Pan YT. (2014). EBSD investigation on microstructure transformation in low carbon steel during continuous cooling. Canadian Metallurgy Quarterly, 53(3):352-361.

[8] Kop TA., Sietsma J., and van der Zwaag S. (2001) Dilatometric analysis of phase transformations in hypo-eutectoid steels. Journal of Material Science, 36: 519-526.

[9] Petrov R., Kestens L., and Houbaert Y. (2004). Characterization of the microstructure and transformation behavior of strained and non-strained austenite in Nb-V-alloyed C-Mn steel. Materials Characterization, 53:51–61.

[10] Manohar PA., Chandra T., and Killmore CR. (1996). Continuous cooling transformation behaviour of micro-alloyed steels containing Ti, Nb, Mn and Mo. ISIJ International Journal, 36(12): 1486–1493.

[11] Jenney CL, O'Brien A. (2001). Welding Handbook. Welding Science and Technology Vol. 1. American Welding Society.

[12] Mayr P. (2007). Evolution of microstructure and mechanical properties of the heat affected zone in B-containing 9% chromium steels. PhD Thesis. Faculty of Mechanical Engineering, Graz University of Technology, Austria.

[13] Ding Q, Wang T, Shi Z, Wang Q, Wang Q, and Zhang F. (2017). Effect of welding heat input on the microstructure and toughness in simulated CGHAZ of 800 MPa Grade steel for hydropower penstocks. Metals; 7(4):115.

[14] Azhari F, Al-Amin Hossain A, Heidarpour A, Zhao XL, and Hutchinson CR. (2018). Mechanical response of ultra-high strength (Grade 1200) steel under extreme cooling conditions. Constructional Building Materials; 175:790–803.

[15] Śloderbach Z. and Pająk J. (2015). Determination of ranges of components of heat affected zone including changes of structures. Archives of metallurgy and materials, 60(4):2607-2612.

[16] Tian Y., Wang H.T., Li Y., Wang Z.D. and Wang G.D. (2017). The analysis of the microstructure and mechanical properties of low carbon microalloyed steels after ultra fast cooling. Materials Research, 20(3):853-589.

[17] Liu X. (2017). Structural effects of welding onto high strength S690 steel plates and welded sections. PhD Thesis, The Hong Kong Polytechnic University.

[18] Liu X, Ho HC, and Chung KF. (2017). Strength reduction of S690-QT welded sections under various heat input energy. Fifteenth East Asia-Pacific Conference on Structural Engineering and Construction (EASEC-15), 11 ~ 13 October 2017, Xi'an, China. (Paper No.: P1412).

[19] Liu X, Chung KF, Ho HC, Xiao M, Hou ZX, and Nethercot D A. (2018). Mechanical behaviour of high strength S690-QT steel welded sections with various heat input energy. Engineering Structures, 175: 245-256.

[20] Wang K, and Chung KF. (2017). Study on structural behaviour of high strength Steel S690 welded H-sections under axial compression. Fifteenth East Asia-Pacific Conference on Structural Engineering and Construction (EASEC-15), 11 to 13 October 2017, Xi'an, China. (Paper No.: P1541).

[21] Ma TY, Liu X, Hu YF, Chung KF and Li GQ. (2017a). Structural behavior of slender columns of high-strength Q690 steel welded H-sections under compression, Engineering Structures, 157, 75-85, February 2018.

[22] Ma TY, Li GQ and Chung KF. (2017b) Numerical investigation into high strength Q690 steel columns of welded H-sections under combined compression and bending. Journal of Constructional Steel Research, 144, 119-134, May 2018.

[23] Ma TY, Hu YF, Liu X, Li GQ and Chung KF. (2017c). Experimental investigation into high strength Q690 steel welded H-sections under combined compression and bending. Journal of Constructional Steel Research, 138, 449-462, November 2017.

[24] Wang K, Chung KF and Ma TY. (2017). Experimental investigation into lateral torsional buckling of S690 welded I-sections. Fifteenth East Asia-Pacific Conference on Structural Engineering and Construction (EASEC-15), 11 to 13 October 2017, Xi'an, China. (Paper No.: P1537).

[25] AISC (2016). ANSI/AISC 360-16: Specification for Structural Steel Buildings. American Institute of Steel Construction, Chicago, U.S.A.

[26] BS EN ISO 6892-1. (2005). Metallic Materials - Tensile Testing Part 1: Method of test at room temperature. International Organization of Standardization.

[27] Liu X, Chung KF, Ho HC, Xiao M, Hou Z and Nethercot DA. (2018). Mechanical behaviour of high strength S690-QT steel welded sections with various heat input energy. Engineering Structures 175: 245-256.

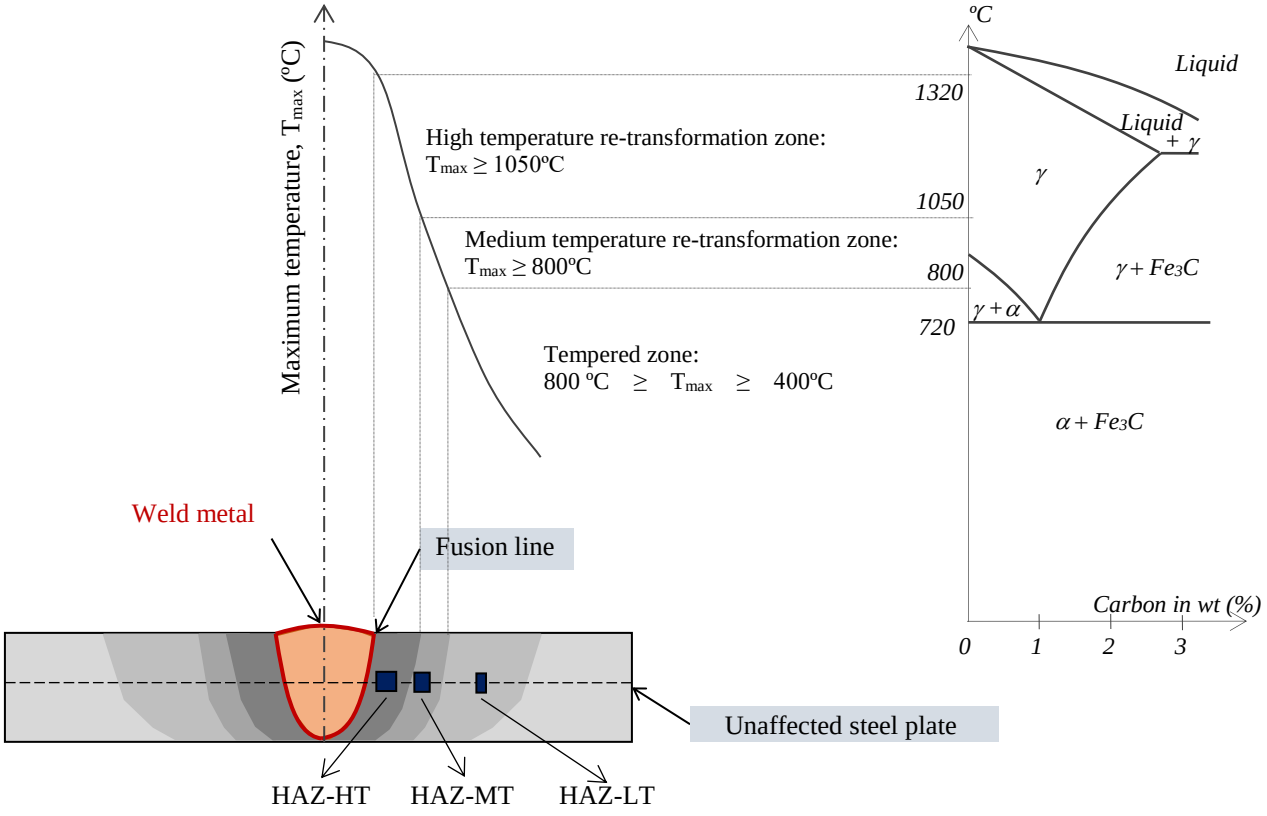

Figure 1 Heat-affected zones in S690 welded sections after a single pass welding

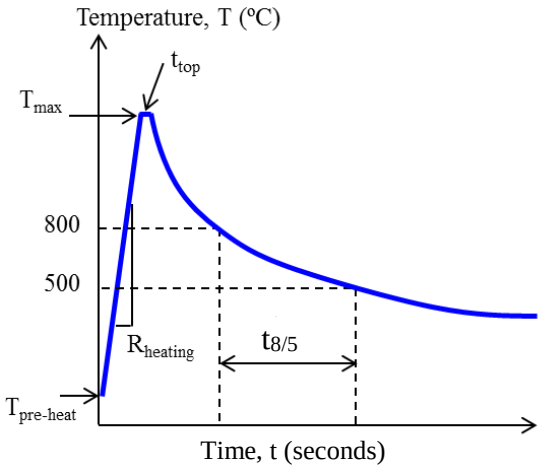

Figure 2 Temperature – time curve of a welded section

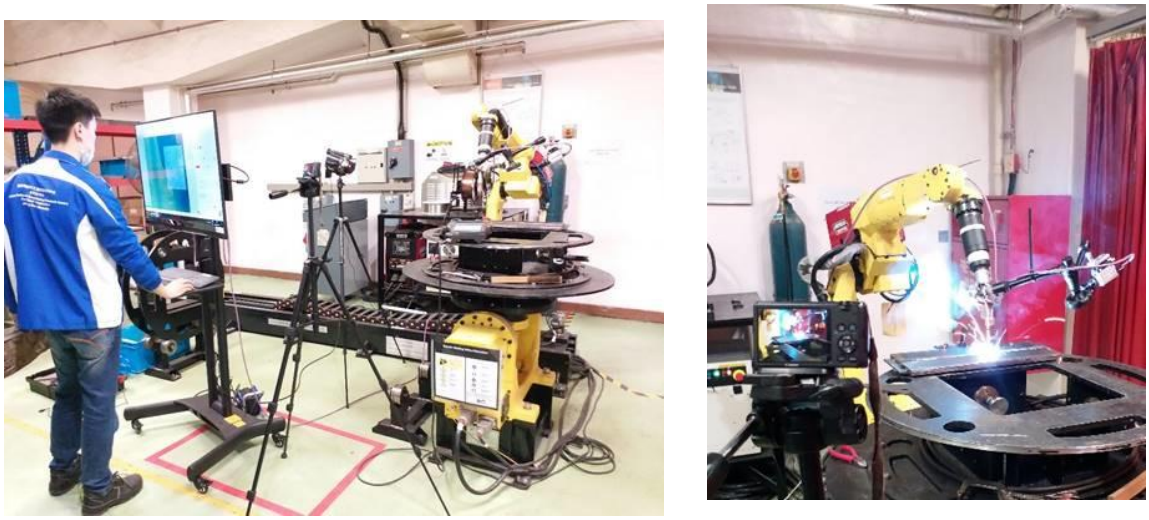

a) In-house robotic welding using a Fanuc-i100 Welding Robot by GMAW

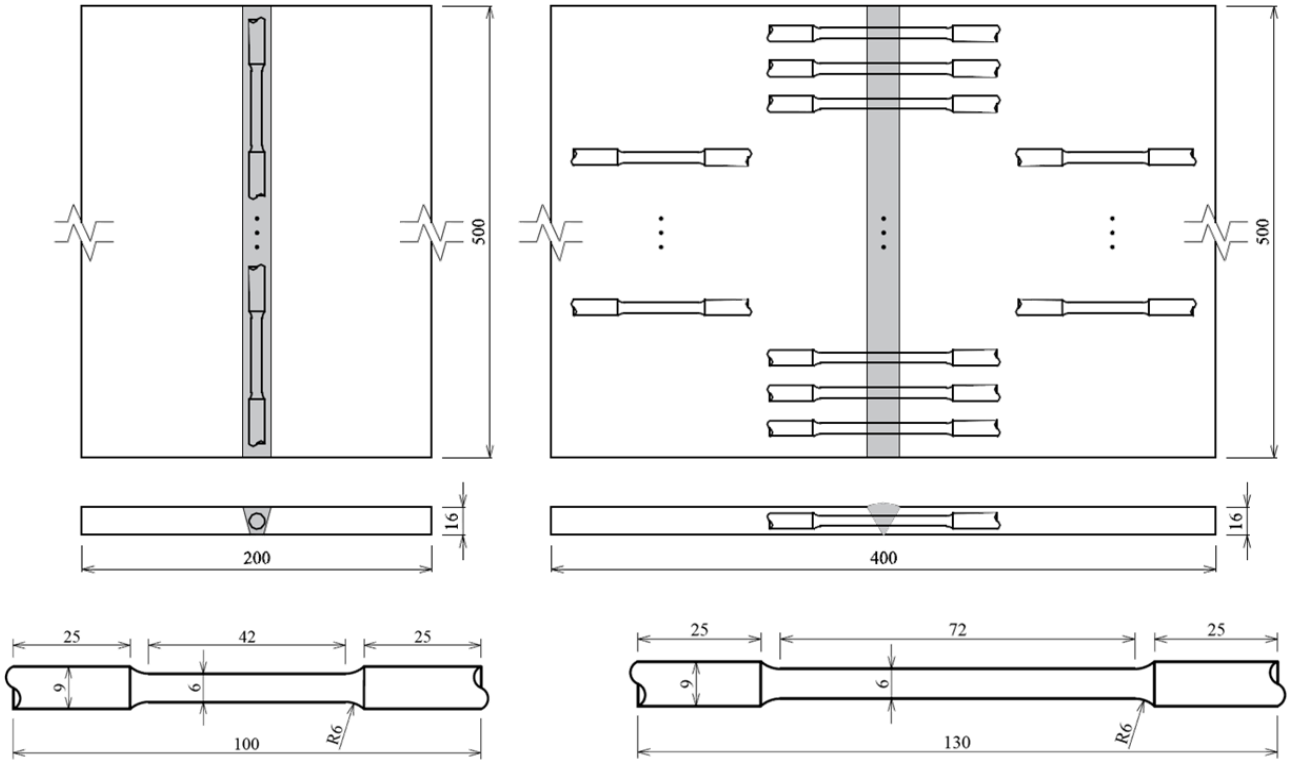

b) Preparation of coupons of steel plates and welded sections

Figure 3 Preparation of welded joints and various coupon types of pilot tests

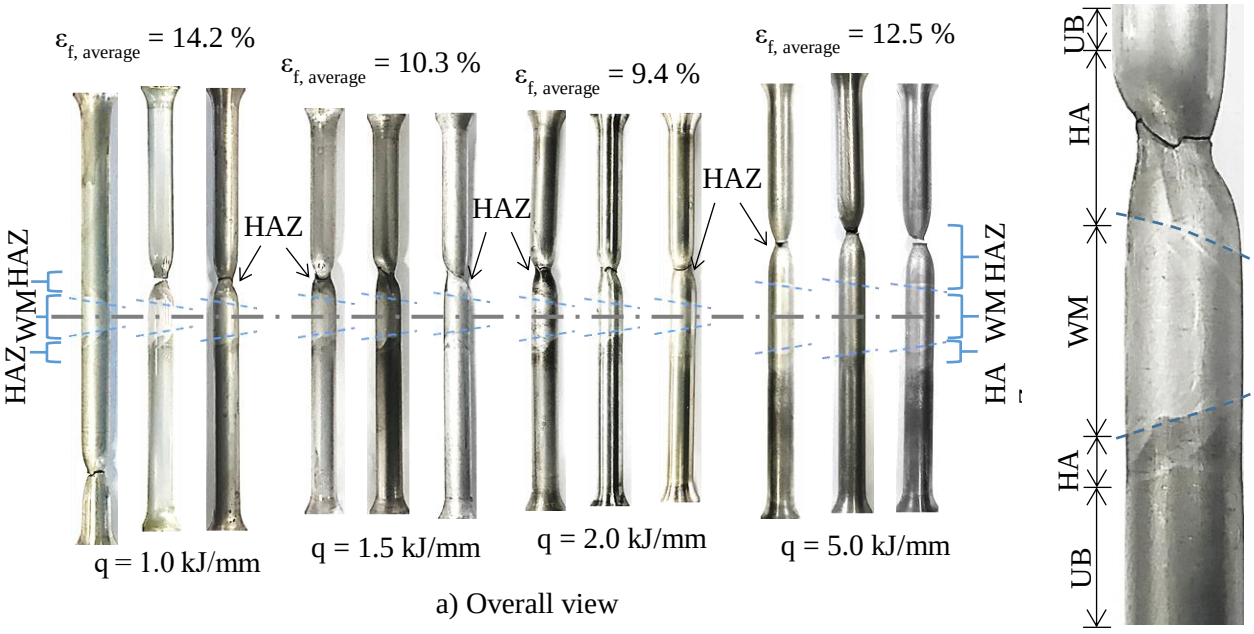

a) Overall view

b) Detailed view

Boundary of the weld metal

WM Weld metal

HAZ Heat affected zone

UB Unaffected base material

Figure 4 Fracture of tensile test coupons

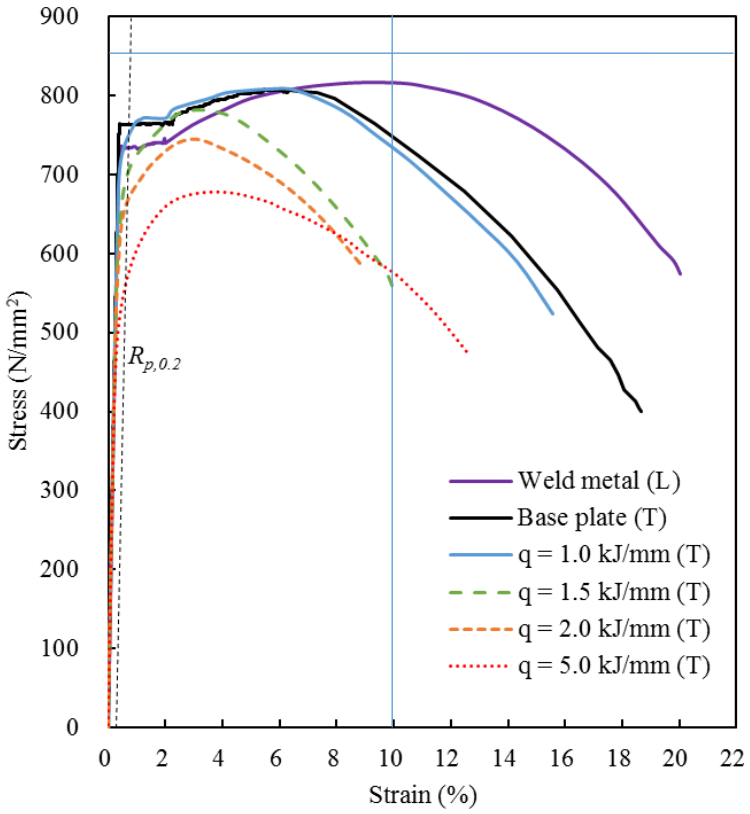

Figure 5 Stress-strain curves of cylindrical coupons of S690 welded sections with different heat input energy q

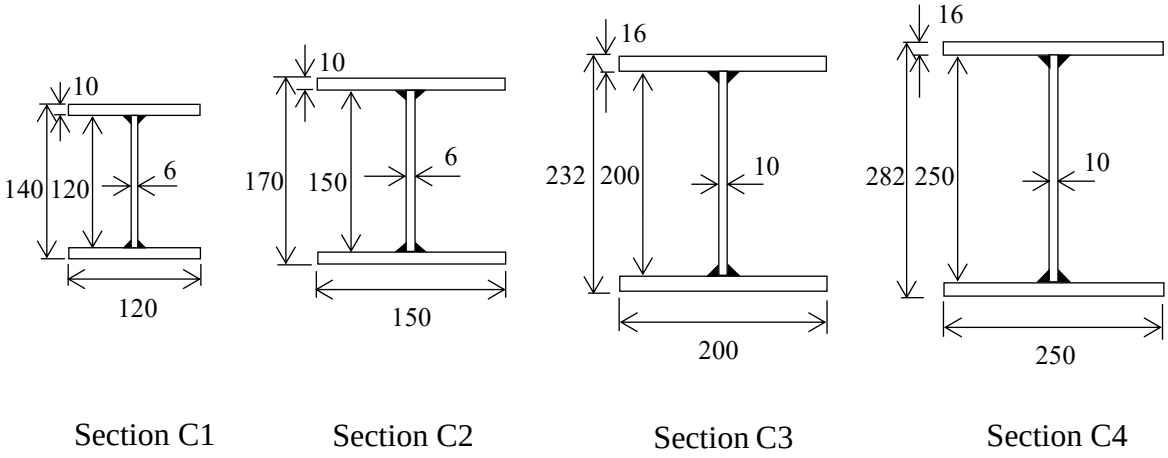

Figure 6 Nominal cross sectional dimensions of high strength S690 steel welded H-sections

a) MTS 400 tons Testing System
(Applied to Sections C1S and C2S)

b) 1000 tons Hydraulic Servo Control Testing System
(Applied to Sections C3S and C4S)

Figure 7 Overview of compression tests on welded H-sections

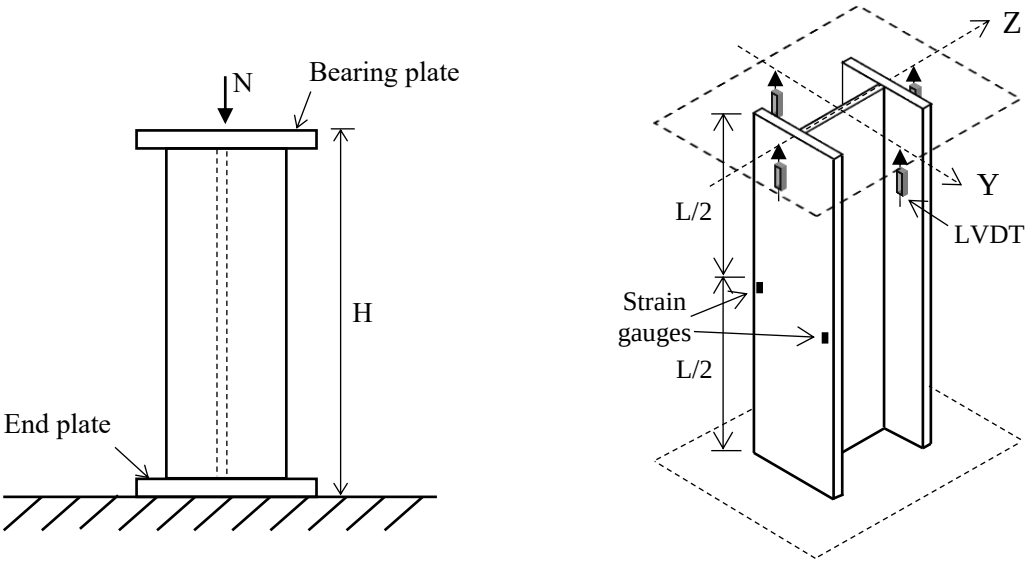

a) Reference welded H-sections

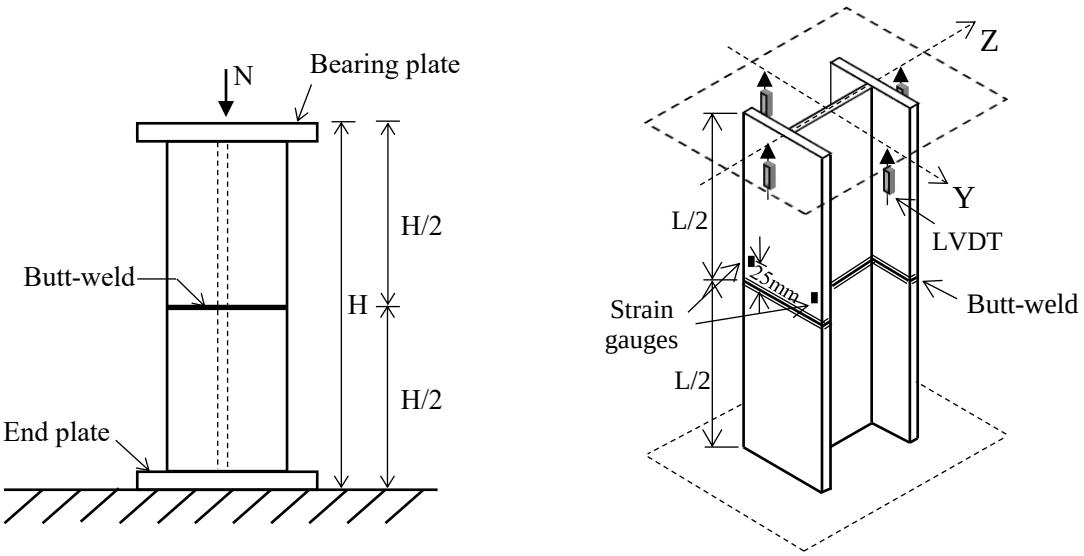

b) Spliced welded H-sections

Figure 8 Test setup for stocky columns under axial compression

 Section C1S-A	 Section C1S-B	 Section C1S-C
 Section C2S-A	 Section C2S-B	 Section C2S-C
 Section C3S-A	 Section C3S-B	 Section C3S-C
 Section C4S-A	 Section C4S-B	 Section C4S-C

Figure 9 Deformed shapes of S690 reference welded H-sections after tests

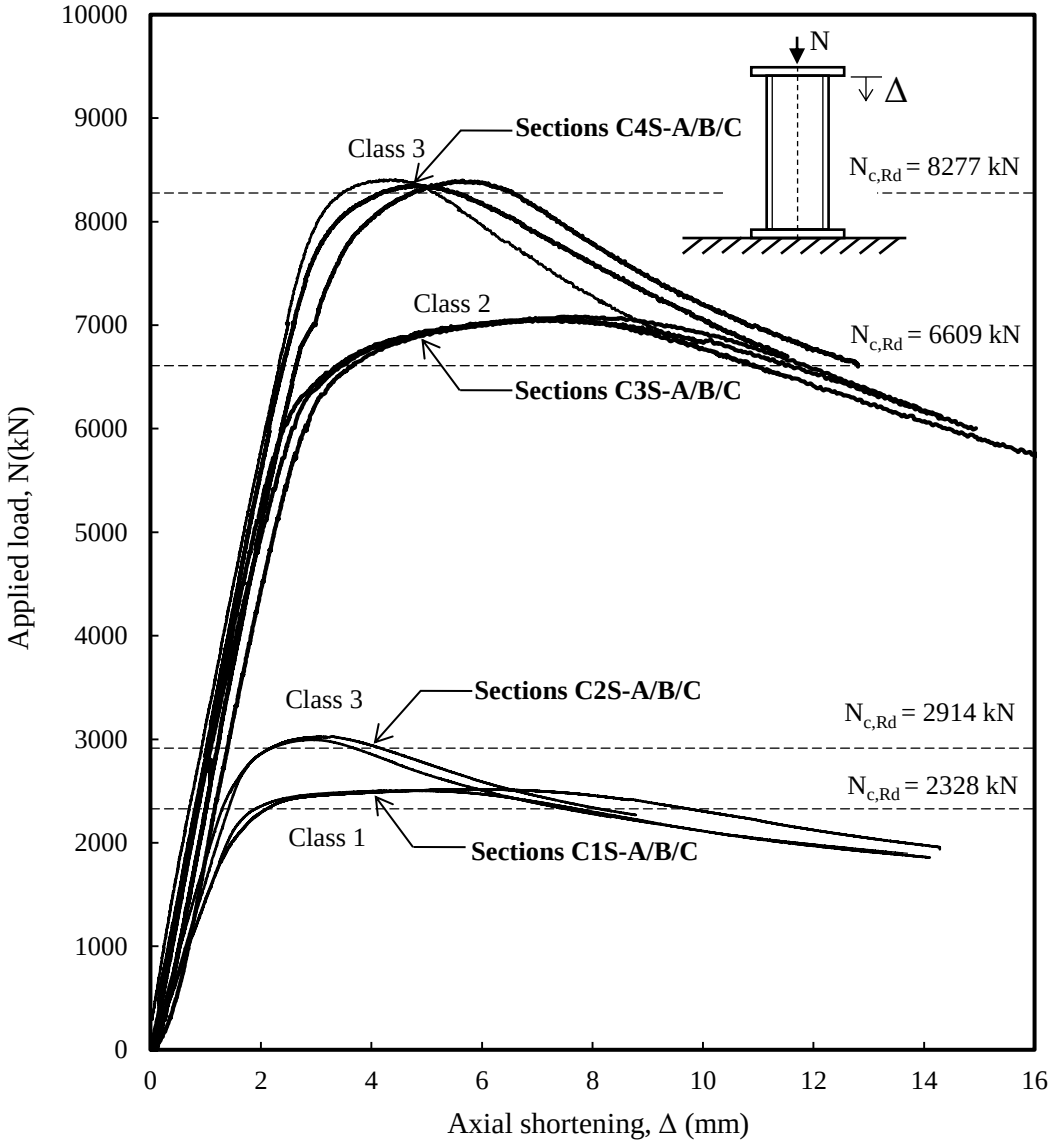

Figure 10 Measured applied load vs axial shortening curves of S690 referenced welded H-sections

Heat input energy, q (kJ/mm)		
1.0	1.5	2.0
 Section C1S-1-bw	 Section C1S-2-bw	 Section C1S-3-bw
 Section C2S-1-bw	 Section C2S-2-bw	 Section C2S-3-bw
 Section C3S-1-bw	 Section C3S-2-bw	 Section C3S-3-bw
 Section C4S-1-bw	 Section C4S-2-bw	 Section C4S-3-bw

Figure 11 Deformed shapes of S690 spliced welded H-sections after tests

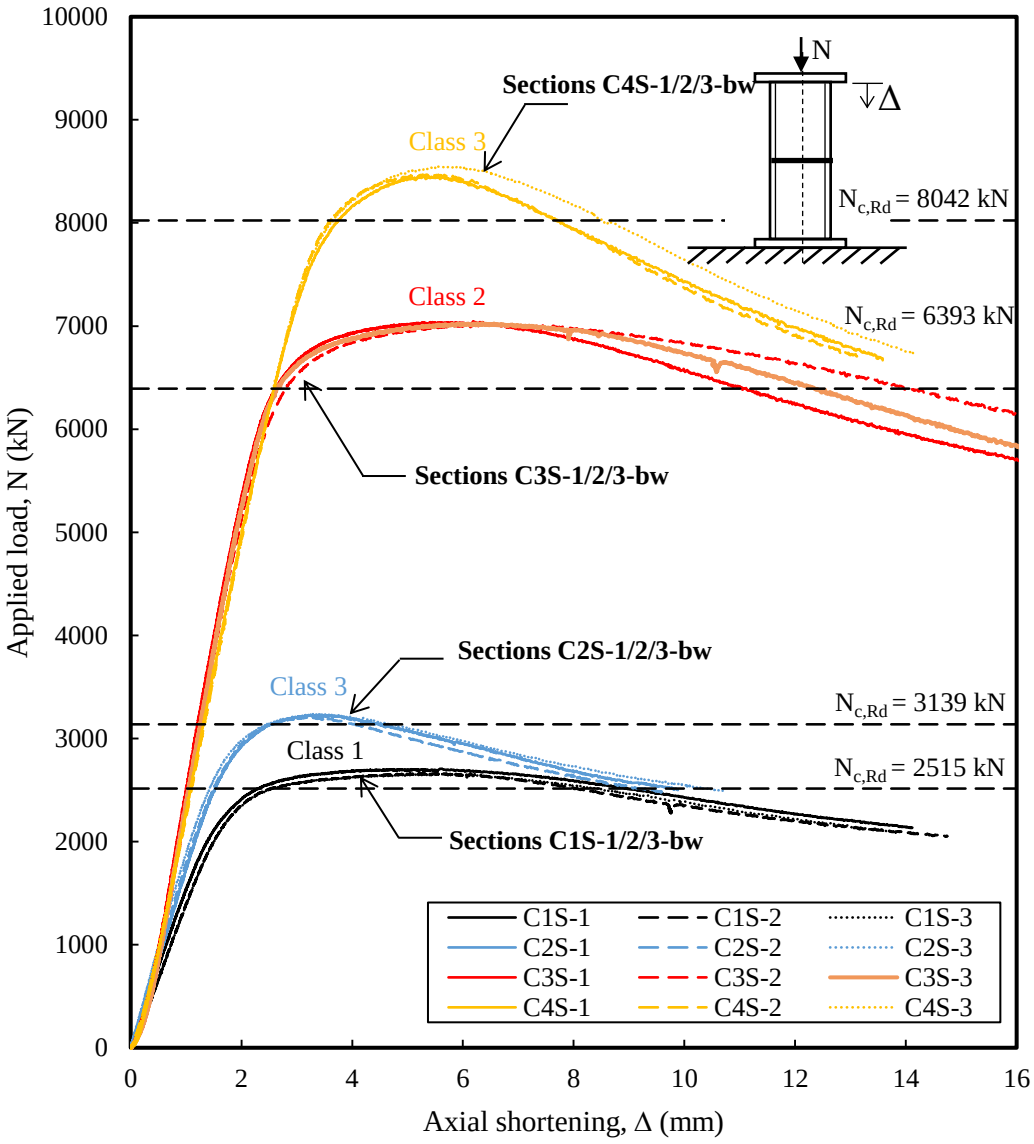

Figure 12 Measured applied load vs axial shortening curves of S690 spliced welded H-sections

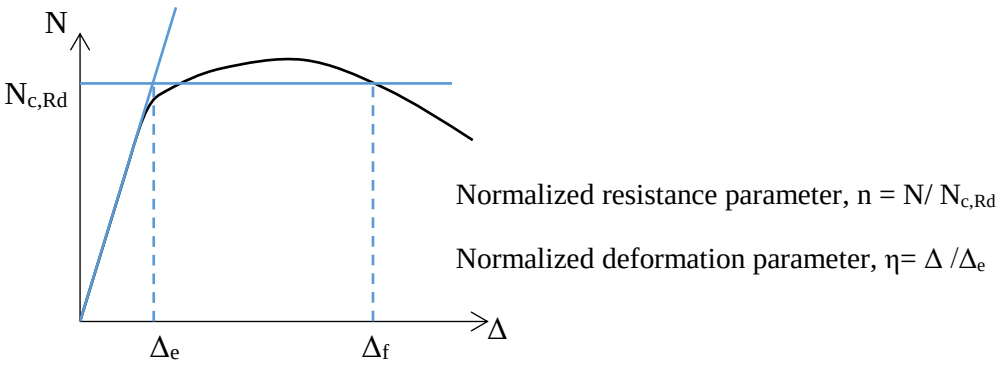

Figure 13 Definition of normalized applied load and normalized axial shortening

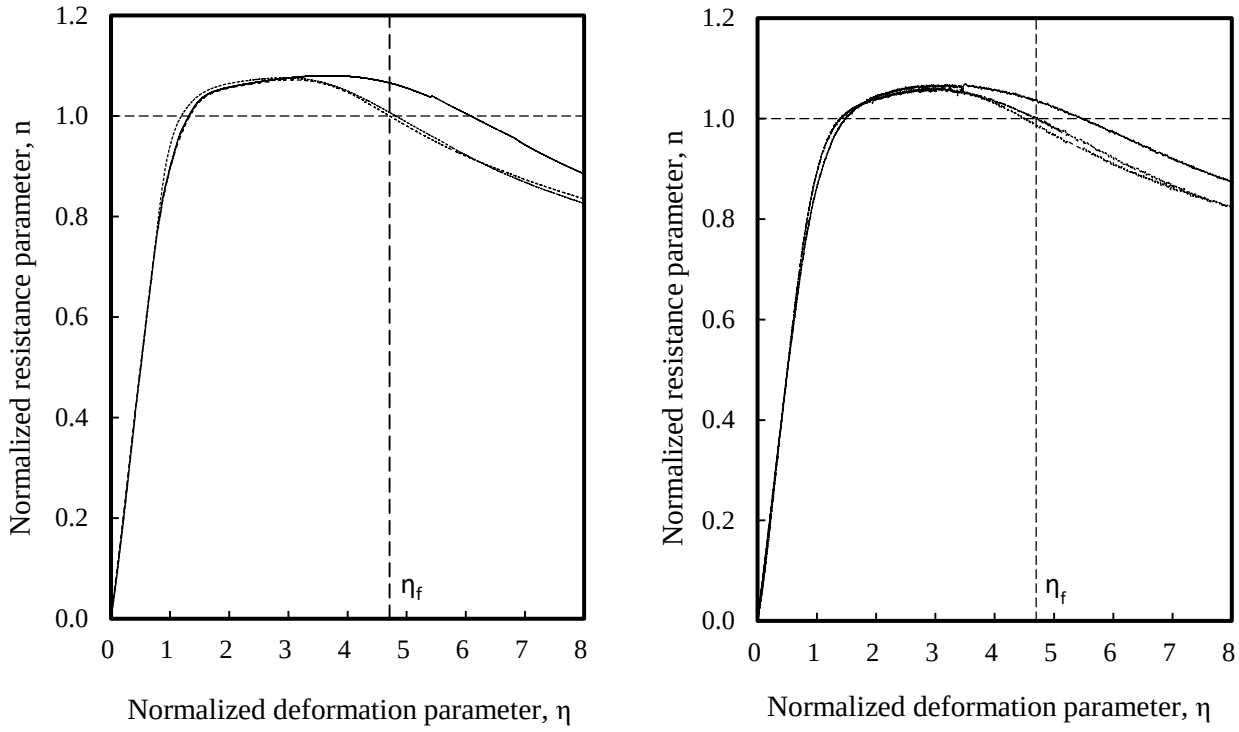

(without butt-weld) *(with butt-welds at mid-height)*

a) **Sections C1S**
Class 1

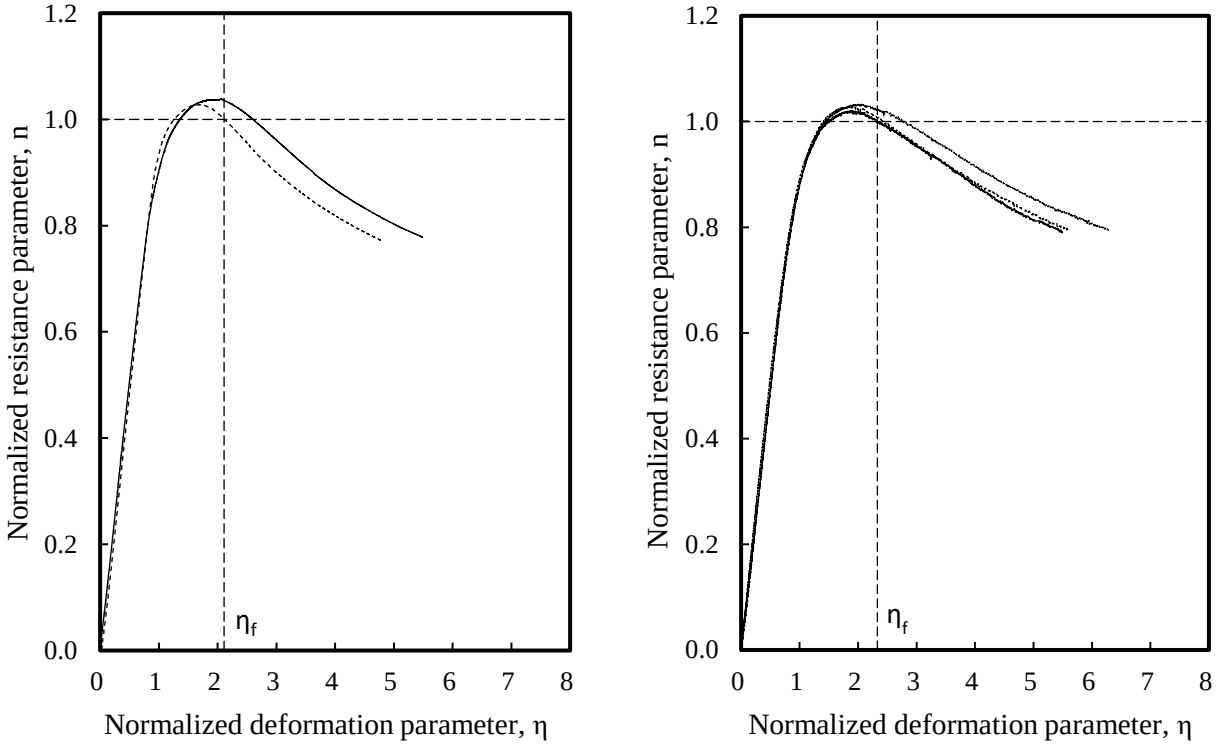

(without butt-weld) *(with butt-welds at mid-height)*

b) **Sections C2S**
Class 3

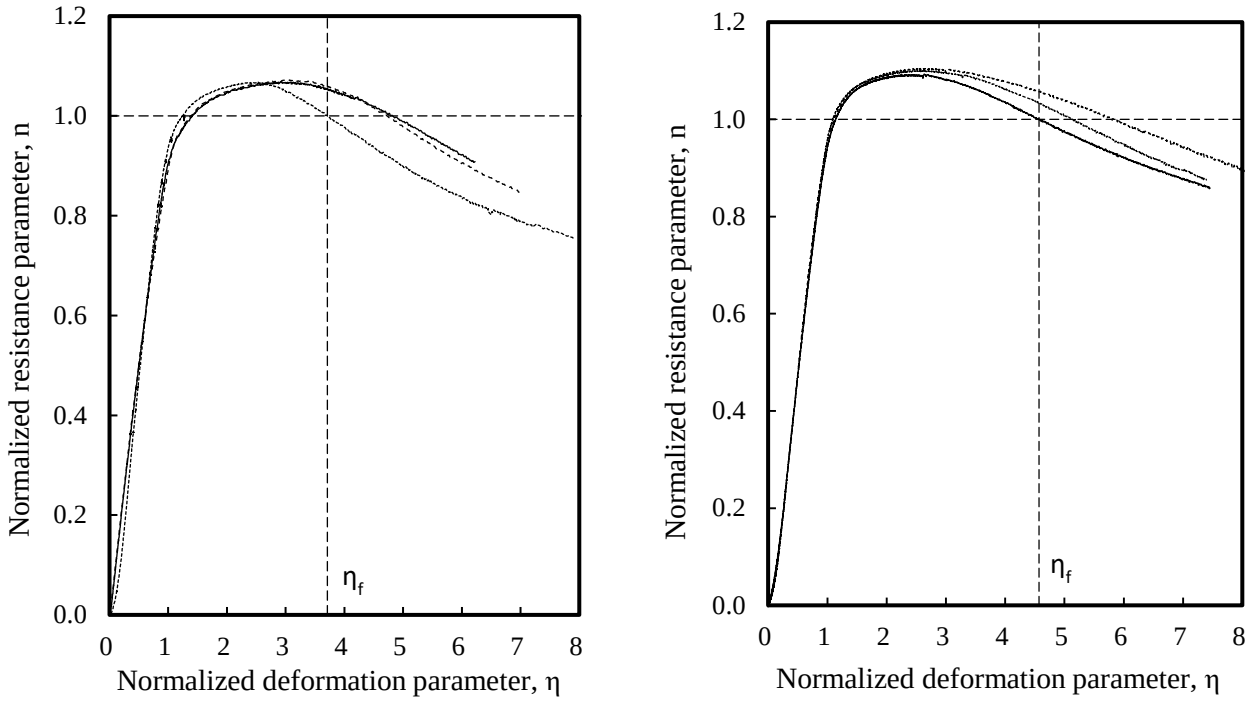

(without butt-weld) *(with butt-welds at mid-height)*

c) **Sections C3S**
Class 2

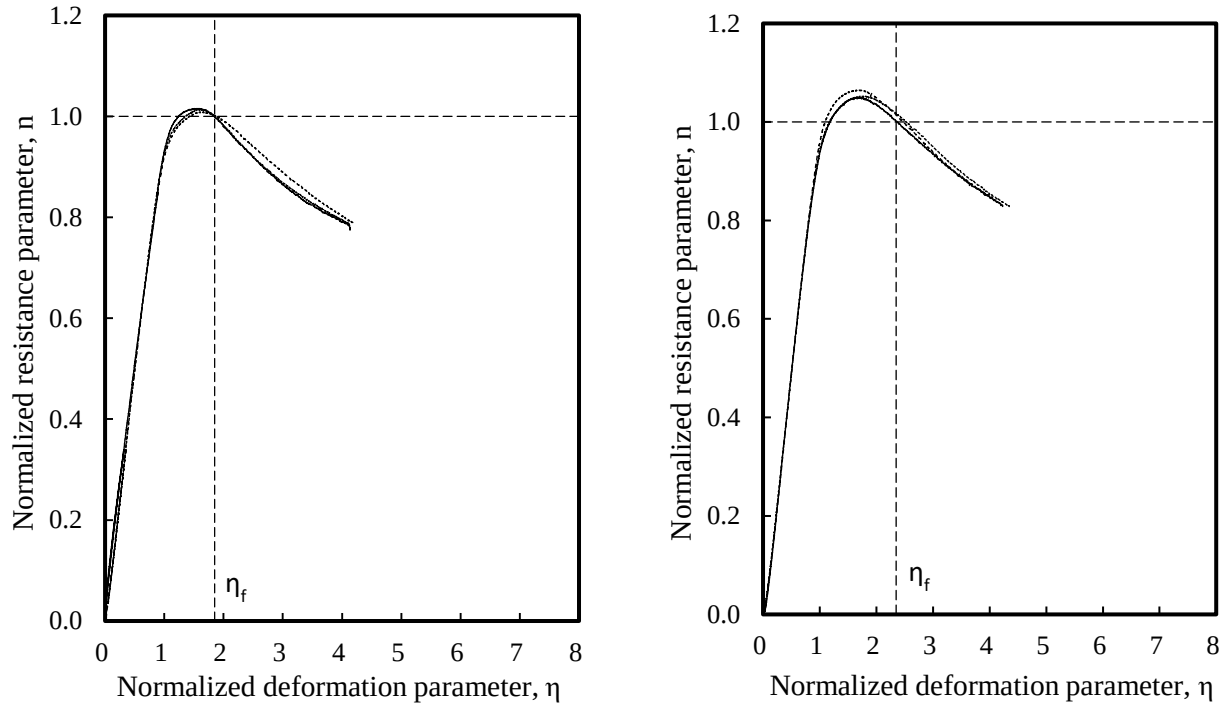

(without butt-weld) *(with butt-welds at mid-height)*

d) **Sections C4S**
Class 3

Figure 14 Comparison on normalized resistance parameter versus normalized deformation parameter of S690 reference and spliced welded H-sections

Table 1 Materials specifications of S690 steels and welding materials

a) Chemical compositions (%)

Material		**C**	**Mn**	**Si**	**S**	**P**	**Cr**	**Ni**	**Mo**	**Cu**
S690 steel plate	-	0.132	1.38	0.25	0.001	0.010	0.28	0.04	0.24	0.47
Welding material	Lincoln 121K3C-H Plus	0.070	1.88	0.29	0.012	0.011	0.07	2.50	0.65	-
	CHW-80C1	0.076	1.86	0.52	0.006	0.007	0.32	2.15	0.60	0.21
	CHW-S80	0.084	1.70	0.18	0.007	0.006	0.45	2.67	0.51	0.05

b) Mechanical properties

Pilot tests – coupons under tension

Plate thickness (mm)	Yield strength f_y (N/mm^2)	Tensile strength f_u (N/mm^2)	Young's modulus E (kN/mm^2)	Strain at tensile strength ε_u (%)	Elongation at fracture ε_L (%)
10	761	810	210	6.85	18.3

S690 reference welded H-sections – stocky columns under compression

Plate thickness (mm)	Yield strength f_y (N/mm^2)	Tensile strength f_u (N/mm^2)	Young's modulus E (kN/mm^2)	Strain at tensile strength ε_u (%)	Elongation at fracture ε_L (%)
6	780	833	215	5.06	19.7
10	754	807	208	5.85	16.2
16	799	855	208	7.53	15.2

S690 spliced welded H-sections – stocky columns under compression

Plate thickness (mm)	Yield strength f_y (N/mm^2)	Tensile strength f_u (N/mm^2)	Young's modulus E (kN/mm^2)	Strain at tensile strength ε_u (%)	Elongation at fracture ε_L (%)
6	722	847	209	6.36	18.8
10	784	874	206	7.42	19.8
16	745	832	216	6.62	19.6

Table 2 Welding parameters for both fillet and butt welds of S690 steels

a) Welding parameters for fillet welds of both S690 reference and spliced welded H-sections

Sections	Plate thickness (mm)	Welding method	Electrode	Welding parameters			
				Voltage U (V)	Current I (A)	Welding speed v (mm/s)	Heat input energy q (kJ/mm)
C1 and C2	6/10	GMAW*	CHW-80C1	30	240	4.0	1.8
C3 and C4	10/16	SAW*	CHW-S80	36	430	5.8	2.7

* By skilled welders.

b) Welding parameters for butt welds of S690 spliced welded H-sections

Plate thickness (mm)	Welding method	Electrode	Welding parameters			
			Voltage U (V)	Current I (A)	Welding speed v (mm/s)	Heat input energy q (kJ/mm)
6	GMAW*	CHW-80C1	20	175	2.9	1.03
			24	220	3.0	1.50
			22	215	2.0	2.01
10			20	170	2.9	1.00
			24	220	3.0	1.50
			24	245	2.5	2.00
16			20	180	3.0	1.02
			21	235	2.8	1.50
			25	280	3.0	1.98

* By skilled welders.

Table 3 Test programme of tensile tests of pilot tests

Steel materials	Coupon type	Heat energy input, q (kJ/mm)	No. of coupons	Welding methods
Steel plate	BP	---	3	---
Welded joints	WS10	1.0	3	GMAW
	WS15	1.5	3	GMAW
	WS20	2.0	3	GMAW
	WS50	5.0	3	SAW
Weld metal	WM	1.0	3	GMAW

Table 4 Welding procedures and parameters for butt welded joints of pilot tests

Welding type	Expected heat input energy (kJ/mm)	Voltage, U (V)	Current, I (A)	Welding speed, v (mm/s)	Efficiency, η	No. of passes	Heat input energy, q (kJ/mm)
GMAW	1.0	28.0	195	4.8	0.85	4	0.97
	1.5	25.9	228	3.3		3	1.52
	2.0	25.9	230	2.5		2	2.03
SAW	5.0	33.0	630	4.0	0.95	1	4.94

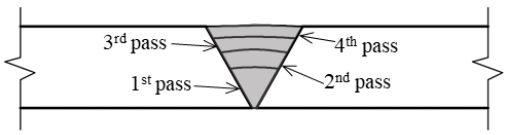

(a) four passes, gap =1 mm → q = 1.0 kJ/mm

GMAW

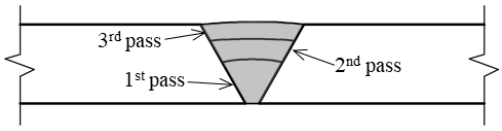

(b) three passes, gap =3 mm → q = 1.5 kJ/mm

GMAW

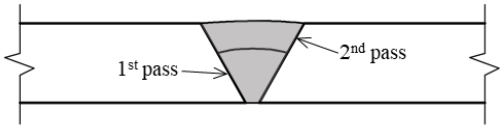

(c) two passes, gap =1 mm → q = 2.0 kJ/mm

GMAW

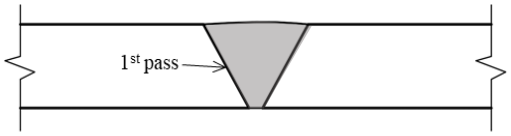

(d) one pass, gap =3 mm → q = 5.0 kJ/mm

SAW

Table 5 Summary of tensile test results of pilot tests

a) Mechanical properties

Specimen	Heat energy input, q (kJ/mm)	E (kN/mm^2)	f_y (N/mm^2)	f_u (N/mm^2)	f_u / f_y	ε_L (%)
BP series	-	210.0	760.9	809.5	1.06	18.3
WS10 series	1.0	208.9	747.8	808.3	1.08	14.2
WS15 series	1.5	210.8	685.9	783.5	1.14	10.0
WS20 series	2.0	207.4	657.2	745.5	1.13	9.4
WS50 series	5.0	203.2	533.2	670.2	1.25	12.5
WM series	1.0	203.7	725.3	815.0	1.12	20.2

b) Reduction factors for mechanical properties

Specimen	Heat energy input, q (kJ/mm)	Reduction factors, α			
		E	f_y	f_u	ε_L
WS10 series	1.0	0.99	0.98	1.00	0.78
WS15 series	1.5	1.00	0.90	0.97	0.55
W20 series	2.0	0.98	0.86	0.92	0.51
WS20 series	5.0	0.97	0.70	0.83	0.68

Notes:

Reduction factor, α for Young modulus = $E / E_{\_BP}$
Reduction factor, α for yield strength = f_y / f_{y_BP}
Reduction factor, α for tensile strength = f_u / f_{u_BP}
Reduction factor, α for elongation = $\varepsilon_f / \varepsilon_{f\_BP}$

Table 6: Test programme and measured dimensions of S690 reference welded H-sections

Specimen	Section classification	h	b_1	b_2	t_{f1}	t_{f2}	t_w^*	H^*	A
		(mm)	(mm)	(mm)	(mm)	(mm)	(mm)	(mm)	(mm^2)
C1S-A	Class 1	137.3	119.6	119.6	9.95	9.95	6.0	460	3084
C1S-B		137.1	119.1	119.1	9.97	9.97			3078
C1S-C		138.3	119.2	119.2	9.96	9.96			3085
C2S-A	Class 3	166.7	149.3	149.3	9.95	9.95	6.0	460	3852
C2S-B		166.2	149.4	149.4	10.00	10.00			3865
C2S-C		167.1	149.3	149.3	9.93	9.93			3849
C3S-A	Class 2	228.3	199.5	199.5	16.02	16.02	10.0	610	8349
C3S-B		230.9	200.2	200.2	16.03	16.03			8401
C3S-C		229.8	200.4	200.4	16.03	16.03			8396
C4S-A	Class 3	283.2	249.9	249.9	16.03	16.03	10.0	760	10516
C4S-B		282.8	250.1	250.1	15.95	15.95			10480
C4S-C		282.9	250.0	250.0	15.95	15.95			10478

Note: * denotes a nominal value.

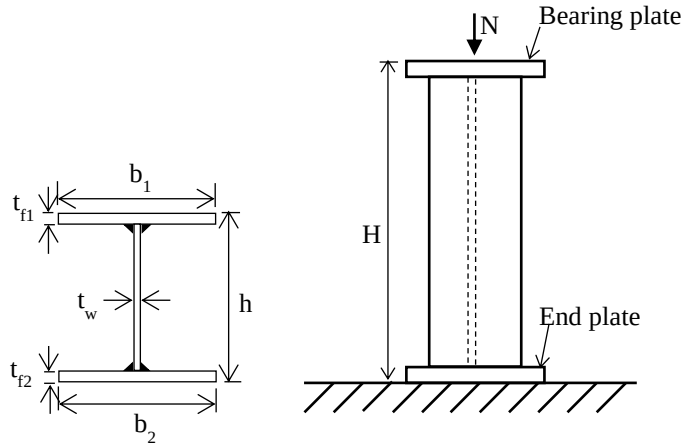

Table 7: Section resistances of S690 reference welded H-sections under compression

Specimen	Section classification	Design resistance $N_{c,Rd}$ (kN)	Measured resistance $N_{c,Rt}$ (kN)	$N_{c,Rt} / N_{c,Rd}$	Δ_e (mm)	Δ_f (mm)	η
C1S-A	Class 1	2330	2515	1.08	1.60	9.73	6.1
C1S-B		2324	2495	1.07	1.60	7.53	4.7
C1S-C		2330	2504	1.07	1.60	7.70	4.8
C2S-A	Class 3	2912	2998	1.03	1.60	4.16	2.6
C2S-B		2920	3029	1.04	1.60	4.16	2.6
C2S-C		2910	2994	1.03	1.74	3.58	2.1
C3S-A	Class 2	6585	7055	1.07	2.95	10.50	3.7
C3S-B		6622	7084	1.07	2.51	11.90	4.7
C3S-C		6620	7066	1.07	2.40	11.56	4.8
C4S-A	Class 3	8297	8384	1.01	2.80	5.17	1.9
C4S-B		8268	8351	1.01	2.95	5.58	1.9
C4S-C		8266	8392	1.02	3.10	5.78	1.9

Table 8: Test programme and measured dimensions of S690 spliced welded H-sections

Specimen	Section classification	h	b_1	b_2	t_{f1}	t_{f2}	t_w^*	H^*	A	Heat input energy, q
		(mm)	(mm)	(mm)	(mm)	(mm)	(mm)	(mm)	(mm^2)	(kJ/mm)
C1S-1-bw	Class 1	140.5	121.5	120.8	10.46	10.75	6.0	460	3285	1.0
C1S-2-bw		140.4	121.3	121.6	10.35	10.55			3255	1.5
C1S-3-bw		140.5	120.5	120.4	10.56	10.51			3254	2.0
C2S-1-bw	Class 3	171.2	151.4	150.7	10.58	10.67	6.0	460	4109	1.0
C2S-2-bw		171.0	149.8	150.1	10.60	10.39			4047	1.5
C2S-3-bw		171.5	150.5	150.3	10.57	10.48			4069	2.0
C3S-1-bw	Class 2	231.4	201.5	200.5	16.28	16.36	10.0	550	8548	1.0
C3S-2-bw		228.2	197.0	198.3	16.25	16.47			8422	1.5
C3S-3-bw		229.3	201.0	201.4	16.15	16.13			8465	2.0
C4S-1-bw	Class 3	283.8	248.6	248.9	16.30	16.52	10.0	760	10674	1.0
C4S-2-bw		285.1	250.0	250.0	16.01	16.05			10545	1.5
C4S-3-bw		281.9	250.7	251.9	16.42	16.53			10770	2.0

Note: * denotes a nominal value.

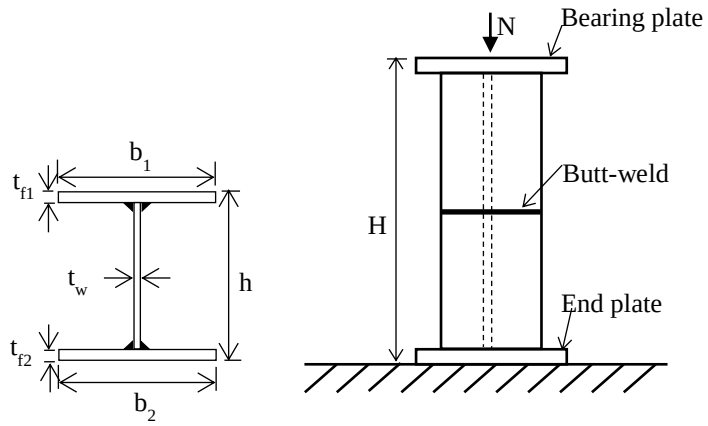

Table 9: Section resistances of S690 spliced welded H-sections under compression

Specimen	Heat input energy q (kJ/mm)	Section classification	Design resistance $N_{c,Rd}$ (kN)	Measured resistance $N_{c,Rt}$ (kN)	$N_{c,Rt}$ / $N_{c,Rd}$	Δ_e (mm)	Δ_f (mm)	η
C1S-1-bw	1.0	Class 1	2531	2707	1.07	1.60	8.75	5.5
C1S-2-bw	1.5		2508	2663	1.06	1.80	8.09	5.1
C1S-3-bw	2.0		2507	2660	1.06	1.80	8.46	4.7
C2S-1-bw	1.0	Class 3	3166	3232	1.02	1.80	4.20	2.3
C2S-2-bw	1.5		3117	3206	1.03	1.72	4.18	2.4
C2S-3-bw	2.0		3134	3240	1.03	1.70	4.74	2.8
C3S-1-bw	1.0	Class 2	6446	7047	1.09	2.35	10.75	4.6
C3S-2-bw	1.5		6351	7022	1.11	2.47	14.40	5.8
C3S-3-bw	2.0		6383	7027	1.10	2.42	12.42	5.1
C4S-1-bw	1.0	Class 3	8050	8453	1.05	3.21	7.60	2.4
C4S-2-bw	1.5		7955	8472	1.06	3.21	7.95	2.5
C4S-3-bw	2.0		8121	8548	1.05	3.25	7.64	2.4

Table 10: Comparison of normalized ductility of welded H-sections under compression

Section	η_f without butt weld	η_f with butt welds at mid-height
Section C1 Class 1	5.2	5.1
Section C2 Class 3	2.4	2.5
Section C3 Class 2	4.4	5.2
Section C4 Class 3	1.9	2.4